4996–5003 *Nucleic Acids Research, 1998, Vol. 26, No. 21*

Circular dichroism and UV melting studies on formation of an intramolecular triplex containing parallel T*A:T and G*G:C triplets: netropsin complexation with the triplex

Claire Gondeau, Jean Claude Maurizot and Maurice Durand*

Centre de Biophysique Moléculaire, Laboratoire affilié à l'Université d'Orléans, Rue Charles Sadron, 45071 Orléans Cedex 2, France

Received May 8, 1998; Revised and Accepted September 2, 1998

ABSTRACT

We have used circular dichroism and UV absorption spectroscopy to characterize the formation and melting behaviour of an intramolecular DNA triple helix containing parallel T*A:T and G*G:C triplets. Our approach to induce and to stabilize a parallel triplex involves the oligonucleotide 5′-d($G_4A_4G_4[T_4]C_4T_4C_4$-$[T_4]G_4T_4G_4$) ($[T_4]$ represents a stretch of four thymine residues). In a 10 mM sodium cacodylate, 0.2 mM disodium EDTA (pH 7) buffer, we have shown the following significant results. (i) While in the absence of $MgCl_2$ this oligonucleotide adopts an intramolecular hairpin duplex structure prolonged by the single strand extremity 5′-d($[T_4]G_4T_4G_4$), the presence of millimolar concentrations of $MgCl_2$ generates an intramolecular triplex (via double hairpin formation). (ii) In contrast to the antiparallel triplex formed by the oligonucleotide 5′-d($G_4T_4G_4[T_4]G_4A_4G_4[T_4]C_4T_4C_4$), the parallel triplex melts in a biphasic manner (a triplex to duplex transition followed by a duplex to coil transition) and is less stable than the antiparallel one. The enthalpy change associated with triplex formation (–37 kcal/mol) is approximately half that of duplex formation (–81 kcal/mol). (iii) The parallel triple helix is disrupted by increasing the concentration of KCl (>10 mM), whereas, under the same conditions, the antiparallel triplex remains stable. (iv) Netropsin, a natural DNA minor groove-binding ligand, binds to the central site A_4/T_4 of the duplex or triplex in an equimolar stoichiometry. Its association constant *K* is smaller for the parallel triplex (~1×10^7 M^{-1}) than for the antiparallel one (~1×10^8 M^{-1}). In contrast to the antiparallel structure, netropsin binding has no apparent effect on thermal stability of the parallel triple helix.

INTRODUCTION

The existence of three-stranded nucleic acid complexes was reported several decades ago (1). The renewed interest in DNA triple helix structures is due to the potential use of oligonucleotides as sequence-specific DNA-binding agents. Thus, the specific recognition of a DNA duplex by short oligonucleotides can be used as a tool for molecular biology (2–4) or as modulators of DNA-binding proteins/gene expression (reviewed in 5). Particularly, it has been shown that formation of a local triple helix may inhibit transcription of a specific gene (6–10).

Several types of triple helix have been characterized which differ according to the composition and orientation of the third strand. The most frequent type involves a pyrimidine-rich third strand which binds parallel to the duplex purine strand by Hoogsteen hydrogen bonding (C^+*G:C and T*A:T triplets; 11–14). One limitation to the formation of the parallel triplets C^+*G:C under physiological conditions is that a slightly acidic pH is required for protonation of the cytosines. Consequently, a second type of triple helix has been developed, involving a purine third strand bound antiparallel to the purine strand of the duplex by reverse Hoogsteen hydrogen bonding (G*G:C and A*A:T triplets; 6,15–19). In recent years, because of the weak stability of short intermolecular triplexes, models of intramolecular structures have been designed (17,20–27). In such structures, shorter stem sequences and lower DNA concentrations can be used, since the interacting components are always in close proximity. Furthermore, the stoichiometry of the three strands and their relative orientations are unambiguously fixed by the construction.

In a recent study, we have investigated formation of a triple helix by oligonucleotide 5′-d($G_4T_4G_4[T_4]G_4A_4G_4[T_4]C_4T_4C_4$) (sequence 2 in Fig. 1) ($[T_4]$ represents a stretch of four thymine residues) by UV absorption spectroscopy and circular dichroism (27). We have demonstrated that in the presence of millimolar concentrations of the divalent cation Mg^{2+}, this oligonucleotide folds back on itself twice to give a short intramolecular triplex via interactions between the 5′-d($G_4T_4G_4$) extremity (which corresponds to a telomeric sequence) and the hairpin duplex counterpart. The design of this oligonucleotide implies that the third strand binds antiparallel to the purine strand of the underlying duplex. This triplex, which contains two $[T_4]$ single-strand loops and non-isomorphic stretches of G*G:C and T*A:T triplets, melts in a monophasic manner. We have shown that the netropsin molecule binds in the minor groove of the central site A_4/T_4 of the underlying duplex in an equimolar

*To whom correspondence should be addressed. Tel: +33 2 38 25 78 58: Fax: +33 2 38 63 15 17; Email: durand@cnrs-orleans.fr

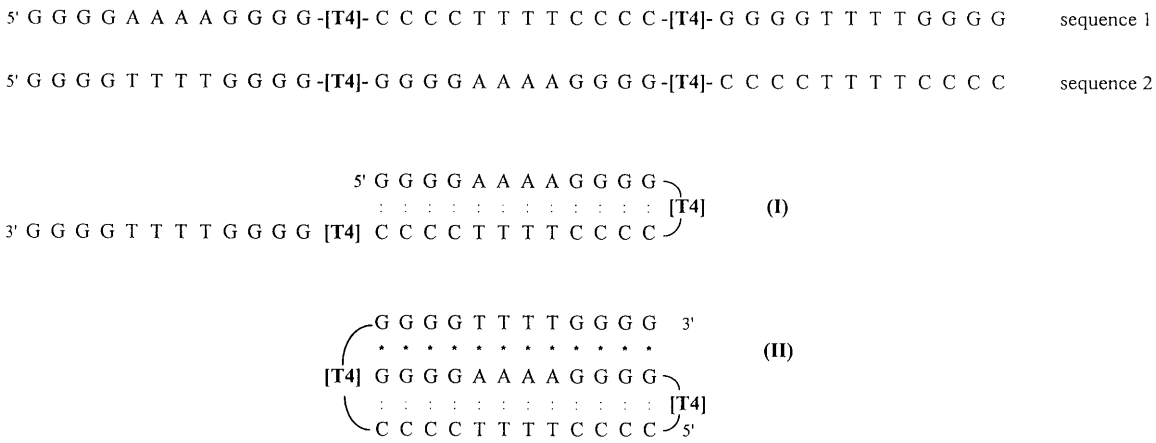

Figure 1. Sequences of oligonucleotides used in the study.

stoichiometry and that, in contrast to previous studies concerning pyr∗pur:pyr triplexes, this ligand binding stabilizes the antiparallel triplex.

It has been demonstrated that (G,T)-containing oligonucleotides bind to double helical DNA in an orientation which is expected to depend on base sequence (28,29). Most reported examples involve antiparallel third strands. Formation of these triple helices usually requires a high divalent cation concentration (30). Moreover, a G-rich oligonucleotide is able to form G quadruplex structures which may interfere with formation of a triple helix (32–34) and makes the study of such structures difficult. In order to investigate the effect of orientation of the third strand with respect to the oligopurine sequence of a DNA double helix, we present a study of intramolecular triple helix formation by oligonucleotide 5′-d($G_4A_4G_4[T_4]C_4T_4C_4[T_4]G_4T_4G_4$) (sequence 1 in Fig. 1). The parallel orientation of the third strand is unambiguously fixed by the construction. For comparison with sequence 2, we studied the effect of the monovalent cation K^+ on triple helix formation and its interaction with netropsin.

MATERIALS AND METHODS

Solution preparation

The synthetic DNA oligonucleotide, purified by ion exchange HPLC, was purchased from Appligene Oncor. It was used after further purification on 15% polyacrylamide gels containing 7 M urea. Oligonucleotide solutions were prepared with a buffer containing 10 mM sodium cacodylate and 0.2 mM disodium EDTA (pH 7) and dialysed against this buffer. The salt concentration of the solutions was adjusted to the desired level by adding a known amount of concentrated solutions of salt. The duplex and triplex solutions of oligonucleotide 5′-d($G_4A_4G_4[T_4]C_4T_4C_4[T_4]G_4T_4G_4$) were incubated at 95°C for 10 min and then cooled back slowly to room temperature before storage at 4°C overnight. The oligomer concentrations, expressed per nucleotide, were determined from high temperature absorbance at 260 nm, i.e. with DNA in the denatured state.

Netropsin (Serva) was used without further purification. Working solutions were prepared daily by dissolving netropsin in buffer. The concentration was determined spectrophotometrically using the molar extinction coefficient ε_{296} = 21 500 $M^{-1}cm^{-1}$.

UV thermal denaturation experiments

The UV absorbance and melting studies were carried out on a Uvikon Kontron 941 spectrophotometer as previously described (27).

Melting temperatures (T_m) were taken as the temperature of half-dissociation of the DNA duplex or triplex and were obtained from the maximum of the first derivative dA/dT plots (where A is absorbance and T is temperature) at 260 nm, except for the triplex to duplex transition of the parallel triplex (280 nm). Indeed, the hyperchromicity is higher at 280 nm than at 260 nm in that case. Precision in T_m values, estimated from variance in three or four repeated experiments, was ±0.5°C, except for the broad triplex to duplex transition of the parallel triple helix structure (±1°C).

Circular dichroism spectroscopy

Circular dichroism (CD) measurements were carried out on a Jobin-Yvon Mark IV dichrograph. Spectral titrations were carried out at 3°C. For denaturation studies, dichroism readings were collected at 5°C intervals. Each CD spectrum was an average of two scans with the buffer blank subtracted, which was also an average of two scans. The concentration used to calculate the CD spectra was that of the nucleotide unit.

Thermodynamic analysis

The enthalpic and the entropic changes (ΔH and ΔS, respectively) corresponding to the biphasic helix–coil transition of the 5′-d($G_4A_4G_4[T_4]C_4T_4C_4[T_4]G_4T_4G_4$) triplex were calculated using a two-state approximation model (the two transitions were analysed separately) as previously described (25).

Determination of equilibrium binding constants

Association constants for netropsin binding to triplexes formed with sequences 1 and 2 were obtained from the changes in the CD signal measured at 314 nm upon addition of netropsin, using the simple site interaction model:

$$L + D \leftrightarrow LD \qquad \mathbf{1}$$

The corresponding association constant K can be written as:

$$K = [LD]/[L][D] \quad \mathbf{2}$$

where [LD] and [L] are the concentrations of bound and free netropsin, respectively, and [D] is the concentration of free oligomer (expressed per oligonucleotide unit). It will be demonstrated that netropsin binds to the studied oligonucleotides in a 1:1 ratio. Thus,

$$[D] = [D]_o - [LD] \quad \mathbf{3}$$

where $[D]_o$ is the total concentration in oligonucleotide. Using an iterative non-linear least squares analysis until the difference in successive iterations was <0.01%, the titration curves were fitted using the association constant *K* and the limiting intensity of the CD signal (asymptotic line) corresponding to a netropsin-saturated oligonucleotide.

RESULTS AND DISCUSSION

Conformations assumed by the oligonucleotide studied in the absence of salt

Temperature-dependent UV absorbance features of the 5′-d(G4A4G4[T4]C4T4C4[T4]G4T4G4) oligonucleotide. In a 10 mM sodium cacodylate, 0.2 mM disodium EDTA (pH 7) buffer, over the entire temperature range available for experimental measurements, the melting profile of sequence 1 is monophasic, cooperative and reversible (T_m = 58°C) (data not shown). No dependence on oligonucleotide concentration, which characterizes intramolecular thermal transition processes, is observed. Taking into account the accuracy in T_m values, we observe no significant difference between the T_m values of sequences 1 and 2 (58 and 57°C, respectively) (27).

CD studies. At low temperature, sequence 1 exhibits a classical B-type CD spectrum, characterized by a wide positive band with three shoulders at 285, 275 and 260 nm followed by a negative band at 242 nm and a positive band at 222 nm (Fig. 2). Around 90°C, the spectrum clearly has a shape corresponding to that of denatured DNA. At 3°C, the spectrum of sequence 1 is close to that of the hairpin duplex form of sequence 2. We note only a difference in the intensity of the wide positive band between 285 and 260 nm.

These results show that, at low temperature, sequence 1 adopts, as does sequence 2 (27), a hairpin duplex structure prolonged by a dangling tail (structure I in Fig. 1). The difference between the CD spectra of the two sequences reflects the importance of the position of the dangling extremity, which prolongs the pyrimidine strand in sequence 1 and the purine strand in sequence 2.

Conformations assumed by the oligonucleotide studied in the presence of $MgCl_2$ salt

Thermal denaturation measurements. Evidence supports intramolecular triplex formation. Using UV spectroscopy, the thermal stability of sequence 1 was monitored at 280 nm in buffer containing increased amounts of $MgCl_2$. After each addition of $MgCl_2$, the solutions were heated for 10 min at 95°C, followed by a slow cooling and incubation at 4°C overnight. It will be demonstrated in the CD studies that a stable equilibrium is attained after this thermal treatment. With a rate of heating/cooling of 0.5°C/min, we noted no hysteresis phenomenon for the

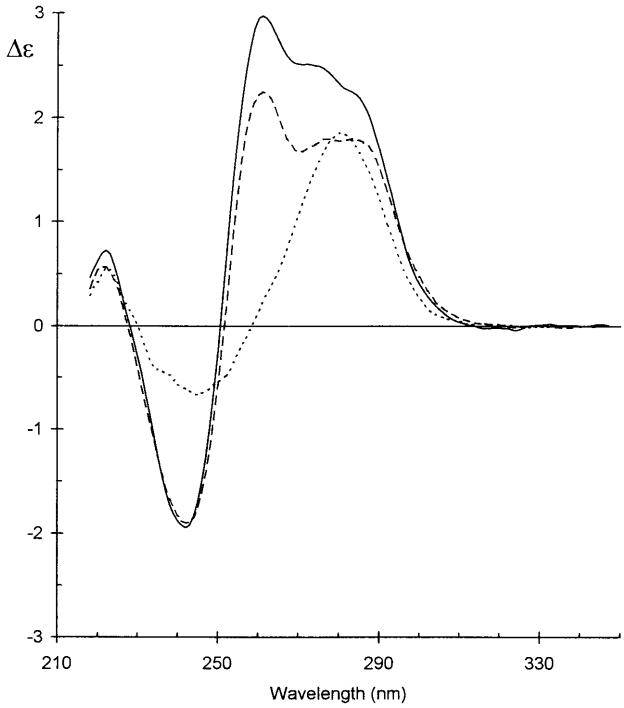

Figure 2. Comparison of the CD spectra of sequences 1 (solid line) and 2 (dashed line) at 3°C and sequence 1 at 90°C (dotted line) in buffer containing 10 mM sodium cacodylate, 0.2 mM EDTA, pH 7.0.

melting profiles. As shown in Figure 3, addition of a small amount of $MgCl_2$ to a solution of the hairpin duplex form of sequence 1 induces a biphasic melting profile. With varying $MgCl_2$ concentrations of from 5 to 150 mM, the T_m of the broad and low temperature transition (first transition) shifts progressively from 24 to 55°C while that of the high temperature transition (second transition) shifts only from 77.5 to 79.5°C. It is noteworthy that addition of 5 mM $MgCl_2$ to a solution of sequence 1 in the hairpin duplex form induces an immediate shift of the second transition from 58 to 77.5°C. We observed the same shift for the hairpin duplex to coil transition of oligonucleotide 5′-d([T_4]$G_4A_4G_4$[T_4]$C_4T_4C_4$), which immediately shifts from 58°C (in the absence of $MgCl_2$) to 78°C in the presence of 5 mM $MgCl_2$. Besides, this transition was almost insensitive to further added $MgCl_2$ (data not shown). Whatever the salt concentration used, we observed no oligonucleotide concentration dependence of the melting curves of sequence 1 (data not shown). This behaviour shows that the two thermal transitions correspond to intramolecular processes. Altogether, these observations allow us to assign the second melting to the hairpin duplex to coil transition and the first melting to the triplex to duplex transition. Regarding the sharpness of the two transitions, we note that, as expected for third strand displacement, the first transition is less cooperative than the second one. It is noteworthy that the parallel triplex structure adopted by sequence 1 is considerably less thermally stable than the corresponding antiparallel triplex formed by sequence 2. Thus, in the presence of 10 mM of $MgCl_2$, the triplex to duplex transition occurs at 28°C with sequence 1 while with sequence 2, the single transition corresponding to a simultaneous

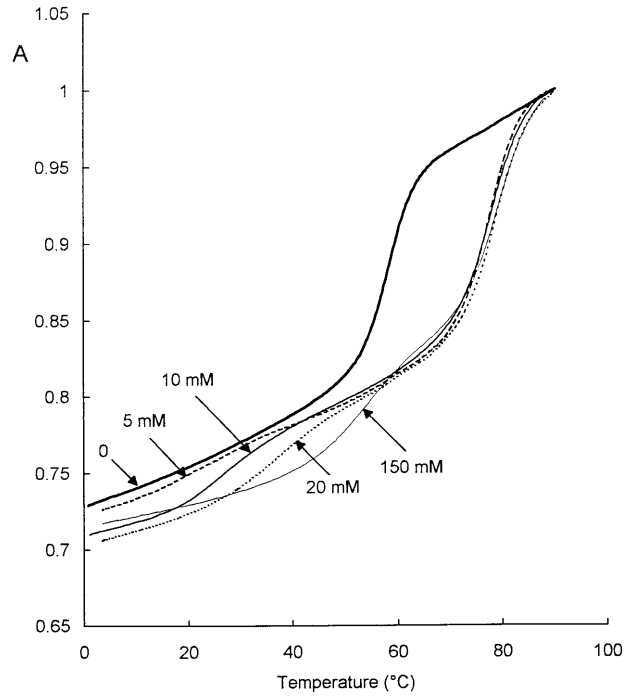

Figure 3. Normalized absorbance versus temperature of sequence 1 for increasing concentration of $MgCl_2$ at 280 nm. [$MgCl_2$], 0 (bold solid line), 5 (dashed line), 10 (solid line), 20 (dotted line) and 150 mM (thin solid line).

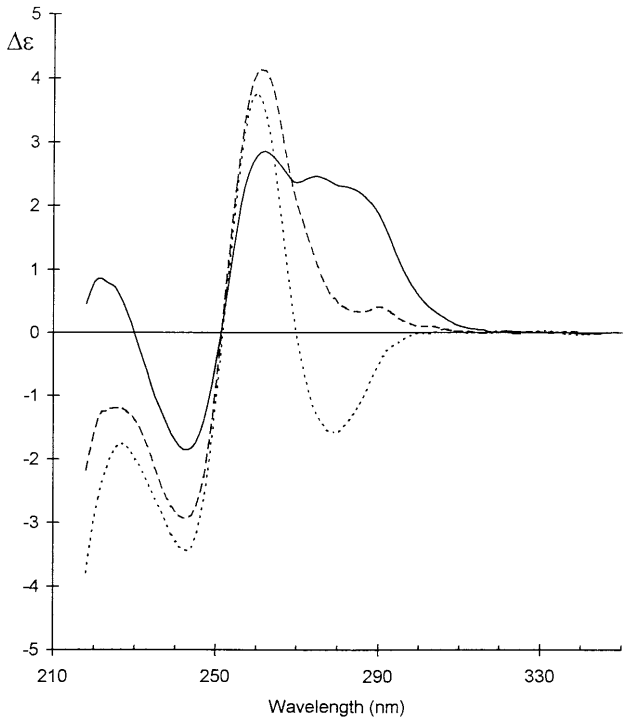

Figure 4. CD spectra at 3°C in the same buffer as in Figure 1 of sequence 1 in the absence of $MgCl_2$ (solid line) and sequences 1 (dashed line) and 2 (dotted line) in the presence of 10 mM $MgCl_2$.

melting of the Watson–Crick and Hoogsteen regions of the triplex is observed at 82°C (27).

For oligonucleotides containing mixtures of G and T residues, molecular modelling studies and footprinting experiments have suggested that the orientation of the third strand depends on the relative number of GpT and TpG steps (28,29). The antiparallel orientation should be favoured for third strands containing more than three GpT and TpG steps; otherwise the parallel orientation should be favoured. In our study, since the hairpin duplexes formed by sequences 1 and 2 contain only one GpA and one ApG step, the parallel triplex should be more stable than the antiparallel one, which is not consistent with our results. Nevertheless, other reports have shown that the polarity of (G,T)-containing third strands depends on the base sequence, on the nature of the bases (modified or not) and on the nature of the salt and the ligand which induce or stabilize the triplex (17,18,30,31,35–40).

CD studies. Based on the results obtained by UV absorption spectroscopy, we performed a CD study of sequence 1 in the presence of 10 mM $MgCl_2$. Figure 4 shows the CD changes observed at 3°C upon addition of 10 mM $MgCl_2$ to a solution of sequence 1 in a hairpin duplex structure. The spectrum of this mixture was recorded at least 3 h after thermal treatment. Indeed, the CD changes are complete after this time. We note an important decrease in the amplitude of the signal at 282 nm and an increase in the negative band at 242 nm, whereas the positive band located at 222 nm disappears, with concomitant appearance of a negative band at 226 nm. This CD spectrum observed in the presence of 10 mM $MgCl_2$ characterizes the parallel intramolecular triplex structure adopted by sequence 1. From 10 up to 150 mM $MgCl_2$, only small additional changes were observed in the CD spectrum, which reflect weak changes in the triple helix structure (data not shown). The significant differences between the CD spectrum of sequences 1 and 2, especially around 280 nm, must be attributed to the orientation of the third strand, which is the only distinction between the two sequences (Fig. 4).

Figure 5 shows the changes in the CD spectrum of sequence 1 with increasing temperature. From 3 to 66°C, the amplitude of the CD band located at 282 nm increases, whereas the negative band located at 226 nm becomes positive. Between 60 and 70°C, the shape of the spectrum changes to that of the duplex structure. Also, the two isoelliptic points detected at 268 and 250 nm reflect a two-state process for the triplex to duplex transition. When the temperature was increased from 66 to 93°C, the CD changes observed reflect the duplex to coil transition, with two isoelliptic points at 229 and 250 nm. The CD spectrum at 93°C clearly has the shape of that of denatured DNA. In accordance with UV experiments, the thermal denaturation profiles monitored at 260 and 280 nm are biphasic (Fig. 5, inset).

KCl effect. The parallel triplex formed by sequence 1 involves binding of the guanine-rich stretch 5′-d($G_4T_4G_4$) to the duplex 5′-d([$G_4A_4G_4$[T_4]$C_4T_4C_4$[T_4]). It is well known that in the presence of K^+, the oligonucleotide 5′-d($G_4T_4G_4$) can self-associate into dimeric structures, forming antiparallel G quadruplexes consisting of two interleaved hairpins with [T_4] loops (41–43). Blume *et al*. (44) showed that inhibition by K^+ of intermolecular pur∗pur:pyr triplex formation by oligo(dG) sequences was dependent upon order of addition of Mg^{2+} and K^+. Thus, we studied the influence of K^+ on stability of the parallel triplex. Upon increasing the concentration of KCl (from 0 to 0.5 M), the shape of the spectrum changes to that of the duplex structure

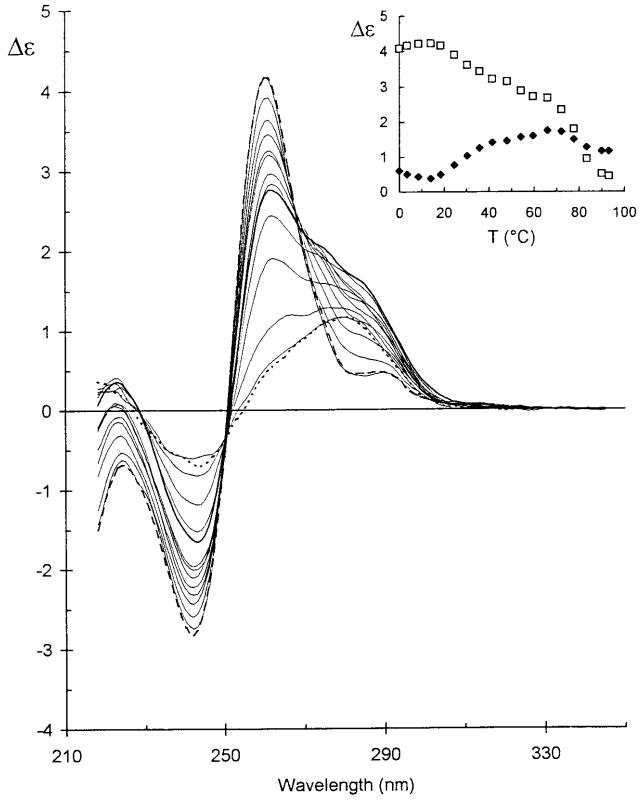

Figure 5. Influence of temperature on the CD spectrum of sequence 1 in the same buffer as in Figure 1 containing 10 mM $MgCl_2$. The temperature varied from 1 to 93°C. The dashed line represents the oligonucleotide at 3°C and the bold solid line the oligonucleotide at 66°C. The oligonucleotide is in a coiled form at 93°C (dotted line). Oligonucleotide concentration was 1.9 µM. The inset corresponds to the melting curves at 260 (□) and 280 nm (◆).

prolonged by the dangling tail 5′-d([T_4]$G_4T_4G_4$), showing that K^+ destabilizes the parallel triplex (data not shown). We observed no disruption of the antiparallel triplex even in the presence of 1 M KCl (27). In order to expose sequence 1 simultaneously to K^+ and Mg^{2+}, a triplex solution containing 10 mM $MgCl_2$ and 0.5 M KCl was heated at 95°C for 10 min followed by cooling to room temperature. The CD spectrum monitored at 3°C 30 min after heating is very close to that recorded before thermal treatment. We conclude that K^+ inhibits formation of a triple helix under these conditions but does not induce formation of particular structures by the telomeric motif 5′-d($G_4T_4G_4$). This result is also in contrast with that obtained with sequence 2 under the same conditions (27).

Thermodynamic analysis of the UV melting curves. In the presence of 10 mM $MgCl_2$, the existence of isoelliptic points in the temperature-dependent CD spectra (Fig. 5) suggests a two-state event for displacement of the third strand (Hoogsteen transition) and denaturation of the hairpin duplex (Watson–Crick transition). Consequently, thermodynamic parameters associated with these transitions were calculated from the UV melting curves using the two-state model previously described (25). For $MgCl_2$ concentrations >10 mM, the proximity of the two transitions does not allow us to calculate the enthalpy and entropy changes associated with the triplex to duplex and duplex to coil processes.

With an accuracy of ±5%, the values of Δ*H* and Δ*S* associated with the triplex to duplex transition are respectively 37 kcal/mol and 124 eu. For the hairpin duplex to coil transition, Δ*H* = 81 kcal/mol and Δ*S* = 232 eu. For the Watson–Crick transition, the absence of an upper baseline makes the analysis difficult. However, taking into account that the thermodynamic parameters can decrease slightly in the presence of salt (25), these values are in accord with those corresponding to hairpin duplex denaturation of sequence 1 in the absence of $MgCl_2$ (Δ*H* = 85 kcal/mol and Δ*S* = 259 eu). The values of Δ*H* and Δ*S* associated with the Hoogsteen transition are approximately half those associated with the Watson–Crick transition. This result matches previous studies on the formation of DNA triplexes by short oligonucleotides (22,39,45,46). This has been attributed to the fact that the opposite phosphate groups in the two parallel chains in the Hoogsteen part of the triplex are in closer proximity than those in the Watson–Crick part and consequently induce higher phosphate–phosphate electrostatic repulsion. The decrease in the entropic barrier for the Hoogsteen interaction can in part be attributed to solvent effects. Positive entropy change being associated with the removal of water from apolar residues, it is possible that there are more water molecules freed upon triplex formation than upon duplex formation.

The parallel triplex formed by sequence 1 contains eight G*G:C and four T*A:T triplets. If one assumes that the loops are thermodynamically neutral (47,48), the mean enthalpy change value for each base binding in the major groove of the underlying duplex is about –3 kcal/mol. This value is similar to that reported by Shchyolkina *et al.* (39) for a parallel DNA triplex containing two non-basic loops and involving five G*G:C and five A*A:T interdispersed triplets (–3.0 kcal/mol in 1 M NaCl). However, Δ*H* values significantly higher than those obtained with sequence 1 were previously reported for Hoogsteen base pair formation: (i) in the buffer used in this experiment, we obtained an enthalpy change of –3.5 kcal/mol with the parallel triplex formed by 5′-d(A_{12}xdT_{12}xdT_{12}) (x is a hexaethylene glycol link) in the presence of 1 M NaCl (25); (ii) with the intermolecular triplex d($C^+_3T_4C^+_3$)·d($G_3T_4G_3$)·d($C_3T_4C_3$) in the presence of 2 M NaCl, Pilch *et al.* (22) reported an enthalpy change of –3.4 kcal/mol. These differences may arise from variations in the base/sequence composition, type of cations, end effects, pH and/or orientation of the third strand relative to the purine strand of the Watson–Crick duplex. Because of the monophasic melting profile obtained with sequence 2 in a previous study (27), it was not possible to compare the enthalpy and entropy changes corresponding to the triplex to duplex transitions associated with the parallel and antiparallel triplexes.

Interaction of netropsin with sequence 1

Netropsin, a natural antibiotic, is known as an AT-specific minor groove-binding ligand. This drug binds in the narrowed minor groove of the B-DNA double helix through a combination of electrostatic interactions with the positive charged ends, hydrogen bonds to N_3 of adenines and O_2 of thymines and van der Waals contacts with the sugar–phosphate backbone at the side walls and floor of the groove (49,50). Data about netropsin–DNA triplex complexes involving T*A:T triplets have been obtained with several techniques (51–53).

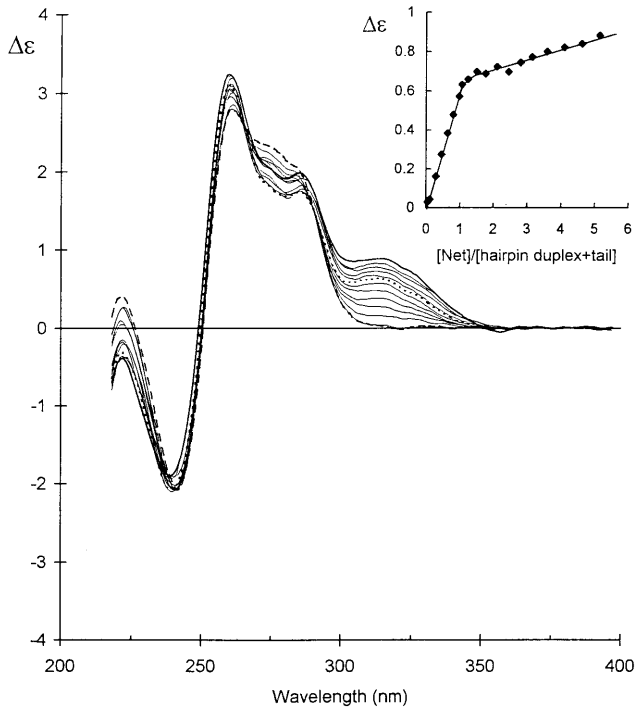

Figure 6. CD spectra of sequence 1 in the absence (dashed line) and in the presence of increasing concentrations of netropsin at 3°C in buffer containing 10 mM sodium cacodylate, 0.2 mM EDTA, pH 7.0. The ratio netropsin:duplex dangling tail (*R*) varied from 0 to 5.2 (solid line). The dotted line corresponds to $R = 1$. Oligonucleotide concentration was 2.1 µM. The inset corresponds to the CD titration curve at 314 nm.

Interaction in the absence of $MgCl_2$. At 3°C, we observe the progressive appearance of a well-defined CD band centred at 314 nm upon incremental addition of netropsin to a solution of sequence 1. The sharp intersection of the two lines in the titration curve followed at 314 nm corresponds to a stoichiometry of 1:1 (netropsin molecule:oligonucleotide) (Fig. 6, inset). For ratios >1, a weak progressive variation in the intensity is observed. There are two modes of interaction in complex formation of netropsin with sequence 1 in the hairpin duplex form. The first binding mode fits with strong affinity for the A_4/T_4 site and the second one with a weaker affinity for the G_4/C_4 site. We obtained similar results with sequence 2 (27). Due to the presence of these two binding modes, the binding constant of netropsin to the A_4/T_4 site was not calculated.

The denaturation process was followed using UV absorbance (data not shown). As expected from studies on duplexes containing only A:T base pairs (51,54,55), the hairpin duplex form of sequence 1 is stabilized by the ligand. The duplex to coil transition was shifted from 58 (in the absence of netropsin) to 82°C (in the presence of netropsin).

Interaction in the presence of 10 mM $MgCl_2$. Figure 7a shows the CD changes observed upon addition of netropsin to sequence 1 at 3°C in buffer containing 10 mM $MgCl_2$. Under these experimental conditions, the free oligonucleotide forms a stable parallel triple helix ($T_m = 28$°C). The appearance of a CD band centred at 314 nm demonstrates interaction between the ligand and the triplex. In the 300–215 nm region, the CD spectrum of the oligonucleotide–netropsin complex has the characteristics of that of sequence 1 in a triple helix structure. Thus the ligand binds to sequence 1 without displacement of the third strand from the major groove, which was confirmed by UV absorption experiments. Intersection of the extrapolated linear part of the titration curve with the limiting intensity of the induced CD signal at 314 nm demonstrates fixation of one netropsin per oligonucleotide (Fig. 7a, inset). The CD difference spectra (compared at a netropsin:oligonucleotide ratio of 1) of the parallel triplex (sequence 1), the antiparallel triplex (sequence 2), both in the presence of 10 mM $MgCl_2$, and the hairpin duplex form of sequence 1 have the same shape in the 350–310 nm region, but the intensities are different (Fig. 7b). In the same wavelength region, the CD difference spectrum of the parallel triplex $d(A_{12}xdT_{12}xdT_{12})$ obtained in 1 M NaCl and that of sequence 1 in the hairpin duplex form are identical (data not shown). This experiment shows that netropsin is located in the minor groove of the central A_4/T_4 site of the triplex, but that its geometry and environment are not exactly identical in the duplex and in the triplex forms. Without detailed structural data about the triplex, it is reasonable to think that the presence of the third strand produces some conformational modifications of the minor groove of the underlying duplex, changing the alignment of the interacting functional groups with the ligand. The structure of the A_4/T_4 site depends on the orientation of the third strand relative to the purine strand and on the nature of the triplets (G∗G:C or T∗A:T) on each side of the binding site.

The increase in the induced CD signal recorded at 314 nm was used to determine ligand association constants (*K*) at 3°C using the analysis given in Materials and Methods. In the presence of 10 mM $MgCl_2$, solid lines fit the titration curves of sequences 1 and 2, using the binding affinities $K \approx 1 \times 10^7\ M^{-1}$ for the parallel triplex and $K \approx 1 \times 10^8\ M^{-1}$ for the antiparallel one (Fig. 7a, inset). Both values correspond to highly specific binding of netropsin to the central A_4/T_4 site. Nevertheless, the significant difference in values demonstrates that netropsin has a higher affinity for the antiparallel triplex.

Denaturation of the netropsin–triplex complex (netropsin: triplex = 4.3) was monitored by UV absorbance spectroscopy at 280 nm (data not shown). The melting profile was biphasic. We observed no significant effect of the ligand on the T_m corresponding to the triplex to duplex transition while that of the duplex to coil transition increases from 78.5 to 87°C. Thus, binding of netropsin has no apparent effect on the stability of the parallel triple helix formed with sequence 1 under the conditions used in this study. In contrast, we observed stabilization of the netropsin–triplex complex with sequence 2 under the same conditions ($T_m = 82$°C in the absence and 87°C in the presence of netropsin). This difference may be explained by the larger binding constant for the antiparallel triplex than for the parallel one. It is noteworthy that in previous studies concerning the interaction between netropsin and the parallel triplex $d(A_{12}xdT_{12}xdT_{12})$, we observed a strong destabilizing effect of the ligand on this structure (51).

CONCLUSION

We have reported experimental evidence that, at low temperature and in the presence of appropriate concentration of $MgCl_2$ (>5 mM), the oligonucleotide 5′-$d(G_4A_4G_4[T_4]C_4T_4C_4[T_4]G_4T_4G_4)$ (sequence 1) folds back on itself twice to form an intramolecular triplex via interaction of the 5′-$d(G_4T_4G_4)$ extremity with the

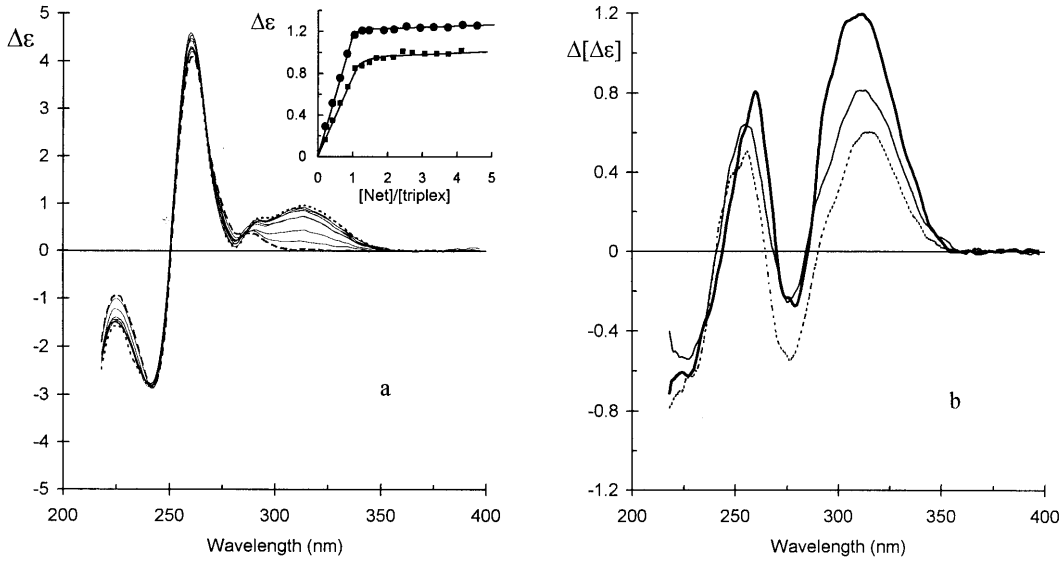

Figure 7. (**a**) CD spectra of sequence 1 in the absence (dashed line) and in the presence of increasing concentrations of netropsin at 3°C in the same buffer as in Figure 6 containing 10 mM $MgCl_2$. The ratio netropsin:triplex (*R*) varied from 0 to 4.3 (dotted line). Oligonucleotide concentration was 2.0 μM. The inset corresponds to the CD titration curves of sequences 1 (■) and 2 (●) at 314 nm. Smooth curves are the least squares fits (details in text). (**b**) Comparison at 3°C and $R = 1$ of the CD difference spectra (expressed in nucleotide units) between the netropsin–oligonucleotide complex and netropsin-free oligonucleotide with sequence 1 in duplex form (dotted line) and with the triplex forms of sequences 1 (thin solid line) and 2 (bold solid line).

hairpin duplex counterpart. The design of this oligonucleotide gives evidence that the third strand binds to the purine strand of the underlying duplex with a parallel orientation through Hoogsteen base pairing, generating non-isomorphic stretches of G∗G:C and T∗A:T triplets. The CD spectrum of this parallel triplex exhibits spectral characteristics which differ from those observed in a previous study of the corresponding antiparallel triplex 5′-d($G_4T_4G_4[T_4]G_4A_4G_4[T_4]C_4T_4C_4$) (sequence 2) (27). In contrast to the single transition observed in the melting profile of the antiparallel triplex, melting studies on the parallel triplex reveal two transitions: the first one represents dissociation of the Hoogsteen domain whereas the second one corresponds to dissociation of the Watson–Crick duplex. The thermal stability of the parallel triplex is remarkably lower than that of the antiparallel triplex ($\Delta T_m = 54°C$ in the presence of 10 mM $MgCl_2$), which illustrates the importance of orientation of the third strand on the stability of triplexes. Moreover, formation of the parallel triplex requires a higher $MgCl_2$ concentration than for the antiparallel one.

Netropsin binds in the minor groove of the underlying duplex of the parallel triplex. It is noteworthy that: (i) netropsin stabilizes the antiparallel triplex but has no apparent effect on stability of the parallel one under the conditions used; (ii) the association constant of netropsin is higher with the antiparallel triplex than with the parallel one.

Binding of (G,T)-containing oligonucleotides in a parallel orientation relative to the purine strand of a duplex often requires a high divalent cation concentration and particular sequences to prevent G quadruplex formation. Thus, the study of this type of triplex is difficult. We have demonstrated in this report that these constraints can be evaded with intramolecular triplexes, which provide useful model systems for studying the stability and structure of short triple-stranded DNAs and their interactions with various ligands. Additionally, the stoichiometry of intramolecular triplexes is perfectly fixed, which is favourable for NMR characterization of structure. Our study complements and extends earlier studies by other authors on the physicochemical behaviour of pur/pyr∗pur:pyr triplexes. The data presented here might be useful in defining the experimental conditions necessary to stabilize triplex DNA and to realize the potential usefulness of triple helices as artificial nucleases and regulators of gene expression *in vitro* and *in vivo*.

REFERENCES

1 Felsenfeld,G., Davies,D.R. and Rich,A. (1957) *J. Am. Chem. Soc.*, **79**, 2023–2024.
2 Ji,H., Francisco,T., Smith,L.M. and Guilfoyle,R.A. (1996) *Genomics*, **31**, 185–192.
3 Pfannschmidt,C., Schaper,A. Heim,G., Jovin,T.M. and Langowski,J. (1996) *Nucleic Acids Res.*, **24**, 1702–1709.
4 Nishikawa,N., Kanda,N., Oishi,M. and Kiyama,R. (1997) *Nucleic Acids Res.*, **25**, 1701–1708.
5 Stull,R.A. and Szoka,F.C.,Jr (1995) *Pharmacol. Res.*, **12**, 465–483.
6 Cooney,M., Czernuszewicz,G., Postel,E.H., Flint,S.J. and Hogan,M.E. (1988) *Science*, **241**, 456–459.
7 Grigoriev,M., Praseuth,D., Guieysse,A.L., Robin,P., Thuong,N.T., Hélène,C. and Harel-Bellan,A. (1993) *Proc. Natl Acad. Sci. USA*, **90**, 3501–3505.
8 Giovannangéli,C., Thuong,N.T. and Hélène,C. (1993) *Proc. Natl Acad. Sci. USA*, **90**, 10013–10017.
9 Hacia,J.G., Dervan,P.B. and Wold,B.J. (1994) *biochemistry*, **33**, 6192–6200.
10 Escudé,C., Giovannangéli,C., Sun,J., Lloyd,D., Chen,J., Gryaznov,S., Garestier,T. and Hélène,C. (1996) *Proc. Natl Acad. Sci. USA*, **93**, 4365–4369.
11 Moser,H.E. and Dervan,P.B. (1987) *Science*, **238**, 645–650.
12 Le Doan,T., Perrouault,L., Praseuth,D., Habhoub,N., Decout,J.L., Thuong,N.T., Lhomme,J. and Hélène,C. (1987) *Nucleic Acids Res.*, **15**, 7749–7760.
13 Rajagopal,P. and Feigon,J. (1989) *Nature*, **339**, 637–640.
14 Radhakrishnan,I. and Patel,D.J. (1994) *Structure*, **2**, 17–32.
15 Pilch,D.S., Levenson,C. and Shafer,R.H. (1991) *Biochemistry*, **30**, 6081–6087.
16 Beal,P.A. and Dervan,P.B. (1991) *Science*, **251**, 1360–1363.

17 Radhakrishnan,I. and Patel,D.J. (1993) *Structure*, **1**, 135–152.
18 Washbrook,E. and Fox,K.R. (1994) *Nucleic Acids Res*., **22**, 3977–3982.
19 Howard,F.B., Miles,H.T. and Ross,P.D. (1995) *Biochemistry*, **34**, 7135–7144.
20 Häner,R. and Dervan,P.B. (1990) *Biochemistry*, **29**, 9761–9765.
21 Sklenar,V. and Feigon,J. (1990) *Nature*, **345**, 836–838.
22 Pilch,D.S., Brousseau,R. and Shafer,R.H. (1990) *Nucleic Acids Res*., **18**, 5743–5750.
23 Chen,F.M. (1991) *Biochemistry*, **30**, 4472–4479.
24 Macaya,R.F., Schultze,P. and Feigon,J. (1992) *J. Am. Chem. Soc*., **114**, 781–783.
25 Durand,M., Peloille,S., Thuong,N.T. and Maurizot,J.C. (1992) *Biochemistry*, **31**, 9197–9204.
26 Völker,J., Botes,D.P., Lindsey,G.G. and Klump,H.H. (1993) *J. Mol. Biol*., **230**, 1278–1290.
27 Gondeau,C., Maurizot,J.C. and Durand,M. (1998) *J. Biomol. Struct. Dyn*., **15**, 1133–1145.
28 Sun,J.S., De Bizemont,T., Duval-Valentin,G., Montenay-Garestier,T. and Hélène,C. (1991) *C.R. Acad. Sci. III*, **313**, 585–590.
29 Giovannangéli,C., Rougee,M., Garestier,T., Thuong,N.T. and Hélène,C. (1992) *Proc. Natl Acad. Sci. USA*, **89**, 8631–8635.
30 Malkov,V.A., Voloshin,O.N., Soyfer,V.N. and Frank-Kamenetskii,M.D. (1993) *Nucleic Acids Res*., **21**, 585–591.
31 Fox,K.R. (1994) *Nucleic Acids Res*., **22**, 2016–2021.
32 Milligan,J.F., Krawczyk,S.H., Wadwani,S. and Matteucci,M.D. (1993) *Nucleic Acids Res*., **21**, 327–333.
33 Cheng,A.J. and Van Dyke,M.W. (1993) *Nucleic Acids Res*., **21**, 5630–5635.
34 Olivas,W.M. and Maher,L.J. (1995) *Biochemistry*, **34**, 278–284.
35 Durland,R.H., Kessler,D.J., Gunnell,S., Duvic,M., Pettott,B.M., Hogan,M.E (1991) *Biochemistry*., **30**, 9246–9255.
36 Radhakrishnan,I., de los Santos,C. and Patel,D.J. (1993) *J. Mol. Biol*., **234**, 188–197.
37 Scaria,P.V., Will,S., Levenson,C. and Shafer,R.H. (1995) *J. Biol. Chem*., **270**, 7295–7303.
38 Kandimalla,E.R., Manning,A. and Agrawal,S. (1996) *J. Biomol. Struct. Dyn*., **14**, 79–90.
39 Shchyolkina,A.K., Borisova,O.F., Minyat,E.E., Timofeev,E.N., Il'icheva,I.A., Khomyakova,E.B. and Florentiev,V.L. (1995) *FEBS Lett*., **367**, 81–84.
40 Escudé,C., Sun,J.S., Nguyen,C.H., Bisagni,E., Garestier,T. and Hélène,C. (1996) *Biochemistry*, **35**, 5735–5740.
41 Scaria,P.V., Shire,S.J. and Shafer,R.H. (1992) *Proc. Natl Acad. Sci. USA*, **89**, 10336–10340.
42 Kang,C.H., Zhang,X., Ratliff,R., Moyzis,R. and Rich,A. (1992) *Nature*, **356**, 126–131.
43 Smith,F.W. and Feigon,J. (1993) *Biochemistry*, **32**, 8682–9692.
44 Blume,S.W., Guarcello,V., Zacharias,W. and Miller,D.,M. (1997) *Nucleic Acids Res*., **25**, 617–625.
45 Plum,G.E., Park,Y.W., Singleton,S.F., Dervan,P.B. and Breslauer,K.J. (1990) *Proc. Natl Acad. Sci. USA*, **87**, 9436–9440.
46 Plum,G.E. and Breslauer,K.J. (1995) *J. Mol. Biol*., **248**, 679–695.
47 Erie,D.A., Sinha,N.K., Olson,W.K., Jones,R.A. and Breslauer,K.J. (1987) *Biochemistry*, **28**, 268–273.
48 Erie,D.A., Sinha,N.K., Olson,W.K., Jones,R.A. and Breslauer,K.J. (1989) *Biochemistry*, **26**, 7150–7159.
49 Kopka,M.L., Yoon,C., Goodsell,D., Pjura,P. and Dickerson,R.E. (1985) *Proc. Natl Acad. Sci. USA*, **82**, 1376–1380.
50 Zimmer,C. and Wähnert,U. (1986) *Prog. Biophys. Mol. Biol*., **47**, 31–112.
51 Durand,M., Thuong,N.T. and Maurizot,J.C. (1992) *J. Biol. Chem*., **267**, 24394–24399.
52 Park,Y.W. and Breslauer,K.J. (1992) *Proc. Natl Acad. Sci. USA*, **89**, 6653–6657.
53 Chalikian,T.V., Plum,G.E., Sarvazyan,A.P. and Breslauer,K.J. (1994) *Biochemistry*, **33**, 8629–8640.
54 Zimmer,C., Luck,G. and Frick,I. (1976) *Nucleic Acids Res*., **3**, 1521–1532.
55 Marky,L.A. and Breslauer,K.J. (1987) *Proc. Natl Acad. Sci. USA*, **84**, 4359–4363.